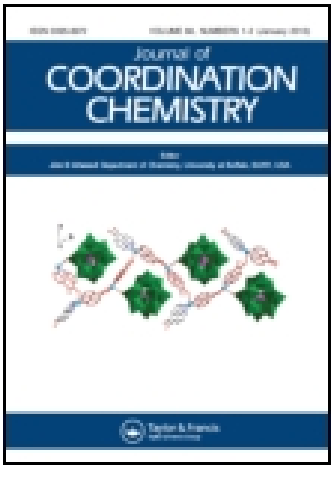

Journal of Coordination Chemistry
Publication details, including instructions for authors and subscription information:
http://www.tandfonline.com/loi/gcoo20

Synthesis, physicochemical characterization, and biological activity of nanocomplexes of iron(III) of 3(2′-hydroxyphenyl)-5-(4-substituted phenyl) pyrazolines and dithiophosphoric acid

U.N. Tripathi[a], A. Siddiqui[a], Kajal Singh[a], Shikha Vishwakarma[a] & Praveen Kumar Mishra[a]
[a] Department of Chemistry, D.D.U. Gorakhpur University, Gorakhpur, India

Accepted author version posted online: 09 Apr 2014.Published online: 09 May 2014.

To cite this article: U.N. Tripathi, A. Siddiqui, Kajal Singh, Shikha Vishwakarma & Praveen Kumar Mishra (2014) Synthesis, physicochemical characterization, and biological activity of nanocomplexes of iron(III) of 3(2′-hydroxyphenyl)-5-(4-substituted phenyl) pyrazolines and dithiophosphoric acid, Journal of Coordination Chemistry, 67:7, 1249-1264, DOI: 10.1080/00958972.2014.911849

To link to this article: http://dx.doi.org/10.1080/00958972.2014.911849

Journal of Coordination Chemistry, 2014
Vol. 67, No. 7, 1249–1264, http://dx.doi.org/10.1080/00958972.2014.911849

Synthesis, physicochemical characterization, and biological activity of nanocomplexes of iron(III) of 3(2′-hydroxyphenyl)-5-(4-substituted phenyl) pyrazolines and dithiophosphoric acid

U.N. TRIPATHI*, A. SIDDIQUI, KAJAL SINGH, SHIKHA VISHWAKARMA and PRAVEEN KUMAR MISHRA

Department of Chemistry, D.D.U. Gorakhpur University, Gorakhpur, India

(*Received 23 July 2013; accepted 26 February 2014*)

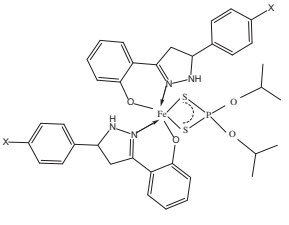

Proposed structure of $Fe(C_6H_{14}O_2PS_2)(C_{15}H_{12}N_2OX)_2$

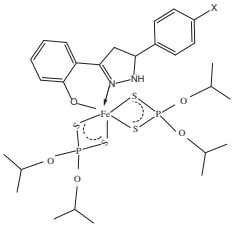

Proposed structure of $Fe(C_6H_{14}O_2PS_2)_2(C_{15}H_{12}N_2OX)$

Complexes of iron(III) with dithiophosphoric acid and 3(2′-hydroxy phenyl)-5-(4-substituted phenyl) pyrazolines, $[Fe(C_6O_{14}O_2PS_2)_2(C_{15}H_{12}N_2OX)]$, and $[Fe(C_6O_{14}O_2PS_2)(C_{15}H_{12}N_2OX)_2]$, where $(C_6O_{14}O_2PS_2H)$ = dithiophosphoric acid, $(C_{15}H_{13}N_2OX)$ = deprotonated 3(2′-hydroxy phenyl)-5-(4-substituted phenyl)pyrazolines (X = H, CH_3, OCH_3, Cl), have been synthesized. These complexes have been physicochemically characterized by elemental analysis (C, H, N, S, Cl, and Fe), magnetic moment data, thermogravimetric analysis, molar conductance, cyclic voltammetry, and spectral analysis (UV–visible, IR, and Fast atom bombardment mass spectrometry). Scanning electron microscopy, TEM, and PXRD have been carried out for powdered samples, which show nanometric particles of these derivatives. Antibacterial and antifungal potential of free pyrazoline and iron(III) complexes have been evaluated.

Keywords: Iron(III); Pyrazolinates; Dithiophosphates; Particle size; Antimicrobial activity

1. Introduction

Pyrazolines are an important class of heterocyclic compounds used in industry as dyes, antioxidants in lubricating oils [1], and in agriculture as catalyst for carboxylation reactions as well as inhibitors for plant growth [2–4] and in photography [5]. Reports are also

*Corresponding author. Email: un_tripathi@yahoo.com

available for a large number of other hydroxy phenyl substituted heterocycles, which are used as agrochemical fungicides [6] and anticonvulsant agents [7]. Complexation behavior of [3(2′-hydroxyphenyl)-5-(4-X-substituted phenyl) pyrazolines with As, Sb, and Bi have been investigated [8–10]. We have also investigated the complexation behavior and antimicrobial potential of 3(2′-hydroxyphenyl)-5-(4-X-phenyl pyrazolines) with tin(IV), organotin(IV), diorganotin(IV), and triorganotin(IV) [11–15].

Iron is a vital element, a deficit of which leads to a decrease in hemoglobin production and results in development of iron deficiency anemia. 3(2′-Hydroxyphenyl)-5-(4-X-phenyl pyrazolines) and substituted pyrazolines with iron(III) have been studied. Synthesis, physicochemical characterization, and biological activity of nanocomplexes of iron(III) of 3(2′-hydroxyphenyl)-5-(4-substituted phenyl) pyrazolines and aspartic acid have also been carried out by Tripathi *et al.* [16]. In this article, we describe synthesis, characterization, and *in vitro* antimicrobial activity of mixed ligand complexes of iron(III) with dithiophosphoric acid and 3(2′-hydroxyphenyl)-5-(4-substituted phenyl) pyrazolines.

2. Experimental

All chemicals were of analytical grade. Solvents were rigorously dried and purified before use by standard procedure [17]. 3(2′-Hydroxyphenyl)-5-(4-substituted phenyl) pyrazolines and dithiophosphoric acid were prepared by reported procedures [18, 19].

2.1. *Synthesis of [Fe($C_6H_{14}O_2PS_2$)($C_{15}H_{12}N_2OX$)$_2$]*

The iron(III) complexes [Fe($C_6H_{14}O_2PS_2$)($C_{15}H_{12}N_2OX$)$_2$] were prepared by the following reaction scheme in two steps:

Step 1 (in 1 : 1 M ratio)

$$FeCl_3 + C_6H_{14}O_2PS_2H \rightarrow FeCl_2(C_6H_{14}O_2PS_2) + HCl\ (\uparrow)$$

Step 2 (in 1 : 2 M ratio)

$$FeCl_2(C_6H_{14}O_2PS_2) + 2(C_{15}H_{13}N_2OX)_2 \rightarrow Fe(C_6H_{14}O_2PS_2)(C_{15}H_{12}N_2OX)_2 + 2\ HCl\ (\uparrow)$$

where $C_6H_{14}O_2PS_2H$ = dithiophosphoric acid, and ($C_{15}H_{13}N_2OX$) = 3(2′-hydroxyphenyl)-5-(4-substituted phenyl) pyrazolines (where X = H, CH_3, OCH_3, Cl).

2.1.1. Synthesis of [Fe($C_6H_{14}O_2PS_2$)($C_{15}H_{12}N_2O{\cdot}OCH_3$)$_2$]. A solution of anhydrous iron (III) chloride (0.47 g, 2.89 mM) in benzene was added dropwise to a slowly stirred benzene solution of dithiophosphoric acid (0.62 g, 2.89 mM) with constant stirring at room temperature, with color change from yellowish brown to gray. The stirring was continued for 7 h and no change in color was observed, indicating completion of the reaction. The product $FeCl_2(C_6H_{14}O_2PS_2)$ was dried under vacuum. The yield was 0.85 g (85%).

The solid thus obtained (0.84 g, 2.45 mM) was dissolved in ethanol. A solution of 3(2′-hydroxyphenyl)-5-(4-methoxy phenyl) pyrazolines (1.33 g, 4.90 mM) was added dropwise to the above solution with constant stirring, with color change from gray to blackish red. The reaction mixture was further stirred for 5 h and there was no further change in color, indicating completion of the reaction. The reaction mixture was dried under vacuum to get blackish red amorphous solid, which was recrystallized in benzene. The yield of $Fe(C_6H_{14}O_2PS_2)(C_{15}H_{12}N_2O{\cdot}OCH_3)_2$ was 1.90 g (95%).

$Fe(C_6H_{14}O_2PS_2)(C_{15}H_{12}N_2OH)_2$, $Fe(C_6H_{14}O_2PS_2)(C_{15}H_{12}N_2OCl)_2$, and $Fe(C_6H_{14}O_2PS_2)(C_{15}H_{12}N_2OCH_3)_2$ were prepared by the same route as described above. The synthetic, physical, and analytical property details are summarized in table 1.

2.2. *Synthesis of $Fe(C_6H_{14}O_2PS_2)_2(C_{15}H_{12}N_2OX)$*

The iron(III) complexes $Fe(C_6H_{14}O_2PS_2)_2(C_{15}H_{12}N_2OX)$ were prepared by the following reaction scheme in two steps:

Step 1 (in 1 : 1 M ratio)

$$FeCl_3 + 2(C_6H_{14}O_2PS_2H) \rightarrow FeCl(C_6H_{14}O_2PS_2)_2 + 2HCl\ (\uparrow)$$

Step 2 (in 1 : 2 M ratio)

$$FeCl(C_6H_{14}O_2PS_2)_2 + (C_{15}H_{13}N_2OX) \rightarrow Fe(C_6H_{14}O_2PS_2)_2(C_{15}H_{12}N_2OX) + HCl\ (\uparrow)$$

where $C_6H_{14}O_2PS_2H$ = dithiophosphoric acid, and $(C_{15}H_{13}N_2OX)$ = 3(2′-hydroxyphenyl)-5-(4′-substituted phenyl) pyrazolines (where X = H, CH_3, OCH_3, Cl).

2.2.1. Synthesis of $[Fe(C_6H_{14}O_2PS_2)_2(C_{15}H_{12}N_2OCl)]$. A solution of anhydrous iron(III) chloride (0.62 g, 1.91 mM) in benzene was added dropwise to a slowly stirred benzene solution of dithiophosphoric acid (1.64 g, 3.82 mM) with constant stirring at room temperature; the color changed from yellowish brown to yellowish gray. The stirring was continued for 9 h and no change in color was observed, indicating completion of the reaction. The product $FeCl(C_6H_{14}O_2PS_2)_2$ was dried under vacuum. The yield was 1.76 g (88%).

The solid thus obtained (1.37 g, 2.65 mM) was dissolved in ethanol. Solution of 3(2′-hydroxyphenyl)-5-(4-chloro phenyl) pyrazoline (0.72 g, 2.65 mM) was added dropwise to the above solution with constant stirring, with color change from yellowish gray to

Table 1. Analytical and physical data for $Fe(C_6H_{14}O_2PS_2)(C_{15}H_{12}N_2OX)$ and $Fe(C_6H_{14}O_2PS_2)_2(C_{15}H_{12}N_2OX)$.

Compound	Yield (%)	M.p. (°C)	Mol. wt. found (Calcd)	Elemental analysis found (Calcd)					
				Fe	C	H	N	S	Cl
$Fe(C_6H_{14}O_2PS_2)(C_{15}H_{12}N_2OH)_2$ (blackish red)	93	135	742 (742.80)	7.54 (7.52)	58.11 (58.16)	5.40 (5.39)	7.55 (7.54)	8.60 (8.62)	–
$Fe(C_6H_{14}O_2PS_2)(C_{15}H_{12}N_2OCl)_2$ (blackish red)	89	142	814 (811.3)	6.90 (6.88)	53.29 (53.25)	4.67 (4.68)	6.89 (6.90)	7.90 (7.89)	8.77 (8.75)
$Fe(C_6H_{14}O_2PS_2)(C_{15}H_{12}N_2OCH_3)_2$ (blackish red)	90	137	768 (770.8)	7.26 (7.24)	59.22 (59.16)	5.70 (5.71)	7.25 (7.27)	8.28 (8.30)	–
$Fe(C_6H_{14}O_2PS_2)(C_{15}H_{12}N_2O{\cdot}OCH_3)_2$ (blackish red)	91	140	802 (804.8)	6.92 (6.94)	56.63 (56.67)	5.48 (5.47)	6.97 (6.96)	7.97 (7.95)	–
$Fe(C_6H_{14}O_2PS_2)_2(C_{15}H_{12}N_2OH)$ (reddish brown)	88	122	720 (718.80)	7.79 (7.77)	45.00 (45.05)	5.72 (5.70)	3.89 (3.90)	17.79 (17.81)	–
$Fe(C_6H_{14}O_2PS_2)_2(C_{15}H_{12}N_2OCl)$ (reddish brown)	92	120	754 (753.30)	7.44 (7.41)	43.08 (43.02)	5.32 (5.31)	3.71 (3.72)	17.00 (16.99)	4.72 (4.71)
$Fe(C_6H_{14}O_2PS_2)_2(C_{15}H_{12}N_2OCH_3)$ (reddish brown)	91	125	733 (732.8)	7.60 (7.62)	45.89 (45.85)	5.88 (5.87)	3.81 (3.82)	17.45 (17.47)	–
$Fe(C_6H_{14}O_2PS_2)_2(C_{15}H_{12}\ N_2O{\cdot}OCH_3)$ (reddish brown)	87	118	750 (749.8)	7.47 (7.45)	44.90 (44.85)	5.74 (5.73)	3.74 (3.73)	17.10 (17.07)	–

reddish brown. The reaction mixture was further stirred for 5 h and there was no further change in color, indicating completion of the reaction. The reaction mixture was dried under vacuum to get reddish brown amorphous solid, which was recrystallized in benzene. The yield of $Fe(C_6H_{14}O_2PS_2)_2(C_{15}H_{12}N_2OCl)$ was 1.88 g (94%).

$Fe(C_6H_{14}O_2PS_2)_2(C_{15}H_{12}N_2OH)$, $Fe(C_6H_{14}O_2PS_2)_2(C_{15}H_{12}N_2O{\cdot}OCH_3)$, and $Fe(C_6H_{14}O_2PS_2)(C_{15}H_{12}N_2OCH_3)_2$ were prepared by the same route as described above. The synthetic, physical, and analytical properties are summarized in table 1.

3. Physical measurements

Chlorine and iron were estimated gravimetrically [17, 20]. The melting point (°C) was recorded on a BI Barnstead electrothermal instrument. The elemental analyses (C, H, and N) were carried out using a model 1 CE-440CHN analyzer. Magnetic moment studies were carried out using a Gouy balance at room temperature. Infrared spectra were recorded using a Varian 3100 FT-IR spectrophotometer from 4000 to 50 cm^{-1}. Fast atom bombardment (FAB) mass spectra were recorded on a JEOL SX 102/DA-600 mass spectrometer. Electronic spectra were recorded in benzene by a UV 1700 series spectrophotometer. Thermogravimetric analyses (TGA) were carried out at a heating rate of 5 °C min^{-1} using an instrument with a Rigaku Thermoflex PTC-10A processor supplied by USIC, Delhi University, New Delhi, India. Molar conductivity was determined in DMSO (1.0×10^{-3} M) at room temperature using a Metrohm 712 conductometer. X-ray diffraction studies of amorphous solids were carried out with a model X'PERT PRO analytical diffractometer at room temperature. Scanning electron microscopy (SEM) images were recorded with a Zeiss EVO microscope operating at 20 kV. The size and shape of the synthesized iron complexes were determined using a JEOL 2010 high-resolution transmission electron microscope operated at 200 kV. The TEM samples were prepared by placing a drop of iron nanoparticle solution on a holey carbon-coated copper grid. Excess solvent was evaporated under argon and the specimen was dried under vacuum. The specific optical rotations were recorded at 25 °C in benzene on a Perkin Elmer model 341 polarimeter using the sodium D line ($\lambda = 589$ nm). Cyclic voltammetry and spectro-electrochemical measurements were performed on a CHI 620c electrochemical analyzer. A glassy carbon working electrode, platinum wire auxiliary electrode, and Ag/Ag + reference electrode were used in a standard three-electrode configuration. Tetrabutylammoniumperchlorate (TBAP) was used as a supporting electrolyte and the solution concentration was 10^{-3} M. A platinum gauze working electrode was used in the spectroelectrochemical experiments.

4. Antimicrobial studies

4.1. *Antibacterial screening*

Antibacterial screening was performed by the disk diffusion method [21, 22]. Nutrient agar (20 mL) was plated in Petri dishes with 0.1 mL of a 10^{-2} dilution of each bacterial culture. Filter paper disks (6 mm in diameter) impregnated with complexes, their ligand, blank, and antibacterial kanamycin were placed on test organism seeded plates. DMSO was used to dissolve the complex and was completely evaporated before application on test organism seeded plates. A blank disk, impregnated with solvent followed by drying, was used as negative control and disks impregnated with antibacterial kanamycin (30 μg per disk) was used

as positive control. Activity was determined after 24 h incubation at 37 °C in a BOD incubator. The diameters of zone of inhibition produced by the complex were then compared with the standard antibiotic kanamycin, 30 μg per disk. Each sample was used in triplicate for the determination of antibacterial activity.

4.2. *Antifungal screening*

Antifungal activities of the complexes were tested by the disk diffusion method [21, 22] against two pathogenic fungi. Filter paper disks (15 mm in diameter) impregnated with complexes and their ligands were placed separately on a Petri plate containing 15 mL potato dDextrose agar. DMSO was used as solvent and was completely evaporated before application on test plates. A blank disk impregnated with solvent, followed by drying, was used as negative control and disks impregnated with antifungal Terbinafin (30 mg per disk) were used as positive control. Mycelial disks of 5 mm diameter, along with the adhering agar cut from the periphery of 7-day old culture with the help of a flame-sterilized cork borer, were placed at the center of the filter paper disk in each plate. The activity was determined after 6 days of incubation at 28 ± 1 °C in a BOD incubator. Each set contained three replicates and observations were recorded on the seventh day in terms of zone of inhibition (mm).

5. Results and discussion

$Fe(C_6H_{14}O_2PS_2)(C_{15}H_{12}N_2OX)_2$ and $Fe(C_6H_{14}O_2PS_2)(C_{15}H_{12}N_2OX)$ are blackish red and reddish brown solids, respectively. They are stable at room temperature and soluble in common organic solvents (benzene, chloroform, acetone, and alcohol) and coordinating solvents (THF, DMF, and DMSO) at slightly elevated temperature. The molecular weight determined by FAB mass spectrum shows monomeric complexes. The elemental analysis (C, H, N, S, Cl, and Fe) data agree with the stoichiometry summarized in table 1.

5.1. *Molar conductance studies*

The molar conductance values of these iron(III) complexes in DMSO at 10^{-3} M were in the range 0.019–0.022 $\Omega\,cm^2\,M^{-1}$. These low values indicate that these complexes are non-electrolytes [23].

5.2. *Magnetic moment measurement*

The effective magnetic moment values for these compounds are 5.78–5.89 BM, corresponding to a high-spin octahedtral [24, 25] geometry. The magnetic moment data are summarized in table 2.

5.3. *Specific optical rotation*

The specific optical rotation values of benzene solution of free pyrazolines and complexes of iron(III) are not measurable at concentrations of 1.00, 0.50, 0.10, and 0.05% due to the dark color of the solution. All the four pyrazolines show zero specific optical rotation at 0.02% concentration. Thus, free pyrazolines are racemic mixtures. The specific optical

Table 2. Electronic spectral and magnetic moment data for $Fe(C_6H_{14}O_2PS_2)(C_{15}H_{12}N_2OX)_2$ and $Fe(C_6H_{14}O_2PS_2)_2(C_{15}H_{12}N_2OX)$.

Complex	Electronic assignment	Spectral band (cm^{-1})	Magnetic moment B.M.
$Fe(C_6H_{14}O_2PS_2)(C_{15}H_{12}N_2OH)_2$	$^6A_{1g}\rightarrow{}^4T_{1g}$	13,530	5.89
	$^6A_{1g}\rightarrow{}^4T_{2g}$	20,009	
	$^6A_{1g}\rightarrow{}^4T_{1g}$	26,525	
	Charge transfer	31,446, 45,871	
$Fe(C_6H_{14}O_2PS_2)(C_{15}H_{12}N_2OCl)_2$	$^6A_{1g}\rightarrow{}^4T_{1g}$	13,621	5.79
	$^6A_{1g}\rightarrow{}^4T_{2g}$	19,950	
	$^6A_{1g}\rightarrow{}^4T_{1g}$	26,509	
	Charge transfer	31,270, 45,789	
$Fe(C_6H_{14}O_2PS_2)(C_{15}H_{12}N_2OCH_3)_2$	$^6A_{1g}\rightarrow{}^4T_{1g}$	13,432	5.85
	$^6A_{1g}\rightarrow{}^4T_{2g}$	20,015	
	$^6A_{1g}\rightarrow{}^4T_{1g}$	26,488	
	Charge transfer	31,498, 46,260	
$Fe(C_6H_{14}O_2PS_2)(C_{15}H_{12}N_2O{\cdot}OCH_3)_2$	$^6A_{1g}\rightarrow{}^4T_{1g}$	13,698	5.87
	$^6A_{1g}\rightarrow{}^4T_{2g}$	19,967	
	$^6A_{1g}\rightarrow{}^4T_{1g}$	26,512	
	Charge transfer	31,367, 45,787	
$Fe(C_6H_{14}O_2PS_2)_2(C_{15}H_{12}N_2OH)$	$^6A_{1g}\rightarrow{}^4T_{1g}$	136,009	5.80
	$^6A_{1g}\rightarrow{}^4T_{2g}$	20,002	
	$^6A_{1g}\rightarrow{}^4T_{1g}$	26,485	
	Charge transfer	31,328, 4584	
$Fe(C_6H_{14}O_2PS_2)_2(C_{15}H_{12}N_2OCl)$	$^6A_{1g}\rightarrow{}^4T_{1g}$	13,618	5.87
	$^6A_{1g}\rightarrow{}^4T_{2g}$	19,923	
	$^6A_{1g}\rightarrow{}^4T_{1g}$	26,490	
	Charge transfer	31,510, 45,792	
$Fe(C_6H_{14}O_2PS_2)_2(C_{15}H_{12}N_2OCH_3)$	$^6A_{1g}\rightarrow{}^4T_{1g}$	13,565	5.81
	$^6A_{1g}\rightarrow{}^4T_{2g}$	21,001	
	$^6A_{1g}\rightarrow{}^4T_{1g}$	26,520	
	Charge transfer	31,473, 46,255	
$Fe(C_6H_{14}O_2PS_2)_2(C_{15}H_{12}N_2O{\cdot}OCH_3)$	$^6A_{1g}\rightarrow{}^4T_{1g}$	135,488	5.78
	$^6A_{1g}\rightarrow{}^4T_{2g}$	19,890	
	$^6A_{1g}\rightarrow{}^4T_{1g}$	26,467	
	Charge transfer	31,446, 45,933	

rotation values for the iron(III) complexes in benzene solution at 0.02% concentration are also zero, indicating that these iron(III) complexes exist as racemic mixtures.

5.4. *Thermogravimetric analysis*

The thermal analysis of $[Fe(C_6H_{14}O_2PS_2)(C_{15}H_{12}N_2OX)_2]$ was performed from 50 to 780 °C under nitrogen. TGA data of these complexes are given in table 3.

All four iron(III) complexes $[Fe(C_6H_{14}O_2PS_2)(C_{15}H_{12}N_2OX)_2]$ show the same kind of decomposition pattern. $[Fe(C_6H_{14}O_2PS_2)(C_{15}H_{12}N_2OOCH_3)_2]$ shows gradual weight loss, indicating decomposition in fragments with increasing temperature. The thermogram exhibits complete decomposition in three steps. The first step occurs between 50 and 379 °C, while the second step takes place between 379 and 540 °C and the third step takes place between 540 and 724 °C. The weight losses are due to elimination of one molecule of dithiophosphoric acid, one molecule of coordinated pyrazolines, and one molecule of coordinated pyrazolines. The remaining residue at 725 °C corresponds to ferric oxide.

Table 3. TGA data of $Fe(C_6H_{14}O_2PS_2)(C_{15}H_{12}N_2OX)_2$.

Complex	Temperature (°C)	Weight loss found (Calcd)	Weight loss between two steps	Fragments lost
$Fe(C_6H_{14}O_2PS_2)(C_{15}H_{12}N_2OH)_2$	390.09	25.08 (27.88)	25.08	$C_6H_{14}O_2PS_2$
	525.32	46.99 (44.80)	22.91	$C_{15}H_{12}N_2OH$
	720.98	83.90 (81.44)	36.91	$C_{15}H_{12}N_2OH$
$Fe(C_6H_{14}O_2PS_2)(C_{15}H_{12}N_2OCl)_2$	400.01	24.01 (26.28)	24.01	$C_6H_{14}O_2PS_2$
	550.12	48.10 (45.16)	24.09	$C_{15}H_{12}N_2OCl$
	730.44	83.99 (82.30)	35.89	$C_{15}H_{12}N_2OCl$
$Fe(C_6H_{14}O_2PS_2)(C_{15}H_{12}N_2OCH_3)_2$	383.77	24.98 (27.08)	24.98	$C_6H_{14}O_2PS_2$
	542.67	47.79 (45.30)	22.81	$C_{15}H_{12}N_2OCH_3$
	745.44	84.50 (82.80)	36.71	$C_{15}H_{12}N_2OCH_3$
$Fe(C_6H_{14}O_2PS_2)(C_{15}H_{12}N_2O{\cdot}OCH_3)_2$	379.29	23.29 (25.08)	23.29	$C_6H_{14}O_2PS_2$
	539.95	48.24 (45.30)	24.95	$C_{15}H_{12}N_2O{\cdot}OCH_3$
	724.51	84.08 (82.90)	37.64	$C_{15}H_{12}N_2O{\cdot}OCH_3$

5.5. *Electronic spectral studies*

The electronic absorption spectral data of high-spin complexes $[Fe(C_6H_{14}O_2PS_2)(C_{15}H_{12}N_2OX)_2]$ and $[Fe(C_6H_{14}O_2PS_2)_2(C_{15}H_{12}N_2OX)]$ in the benzene are summarized in table 2. These iron(III) complexes show absorptions at 13,698–13,488 cm^{-1}, 20,101–19,890 cm^{-1}, 26,525–26,467 cm^{-1}, 31,510–31,270 cm^{-1}, and 45,950–45,787 cm^{-1} assigned to $d \rightarrow d$ transitions arising from the $^6A_{1g} \rightarrow {}^4T_{1g}$ and $^6A_{1g} \rightarrow {}^4T_{2g}$ transitions [26, 27]. These transitions have been reported for octahedral iron(III) complexes. Absorptions at 31,510–31,270 cm^{-1} are assigned to metal to ligand charge-transfer transitions arising from the $d \rightarrow n^*$ transition. Bands at 45,398–46,260 cm^{-1} can be assigned to intraligand, $n \rightarrow n^*$ or $n \rightarrow n^*$ transitions of the pyrazolines and dithiocarbamate [24, 28, 29].

5.6. *Infrared spectral studies*

The infrared spectra of these iron(III) complexes are summarized in table 4. We have studied iron(III) 3(2′-hydroxyphenyl)-5-(4-chloro phenyl) pyrazolinates [26], which show a band at 3365–3342 cm^{-1} assigned to υ(N–H), at almost the same position with respect to spectra of the free pyrazolines, suggesting non-involvement of N–H in bond formation. In all compounds, the band due to υ(C=N) at 1612–1590 cm^{-1} is shifted to lower wavenumber in comparison to spectra of free pyrazolines (at ~1654 cm^{-1}), suggesting coordination

Table 4. IR spectral data for $Fe(C_6H_{14}O_2PS_2)(C_{15}H_{12}N_2OX)_2$ and $Fe(C_6H_{14}O_2PS_2)_2(C_{15}H_{12}N_2OX)$.

Compound	υ (N–H)	υ (C=N)	υ (C–O)	υ ((P)–O–C)	υ (P–O(C))	υ (P=S)	υ (P–S)	υ (Fe–O)	υ (Fe–N)	υ (Fe–S)
$Fe(C_6H_{14}O_2PS_2)(C_{15}H_{12}N_2OH)_2$	3342	1609	–	1170	974	670	550	615	420	335
$Fe(C_6H_{14}O_2PS_2)(C_{15}H_{12}N_2OCl)_2$	3350	1612	–	1175	962	655	552	631	425	361
$Fe(C_6H_{14}O_2PS_2)(C_{15}H_{12}N_2OCH_3)_2$	3346	1598	–	1160	969	664	559	625	433	342
$Fe(C_6H_{14}O_2PS_2)(C_{15}H_{12}N_2O{\cdot}OCH_3)_2$	3351	1600	1028	1152	957	659	551	629	418	350
$Fe(C_6H_{14}O_2PS_2)_2(C_{15}H_{12}N_2OH)$	3359	1592	–	1155	965	668	560	633	425	340
$Fe(C_6H_{14}O_2PS_2)_2(C_{15}H_{12}N_2OCl)$	3365	1605	–	1179	960	682	555	610	430	357
$Fe(C_6H_{14}O_2PS_2)_2(C_{15}H_{12}N_2OCH_3)$	3360	1610	–	1157	955	674	550	619	424	339
$Fe(C_6H_{14}O_2PS_2)_2(C_{15}H_{12}N_2O{\cdot}OCH_3)$	3347	1590	1032	1172	971	664	557	630	427	346

through imino nitrogen. The IR spectra show bands at 633–610 cm^{-1} and 433–418 cm^{-1} which were assigned to υ(Fe–O) and υ(Fe–N), respectively [8, 9, 11–15, 26, 28–31].

The bands at 1028 and 1032 cm^{-1} in $[Fe(C_6H_{14}O_2PS_2)(C_{15}H_{12}N_2OOCH_3)_2]$ and $[Fe(C_6H_{14}O_2PS_2)_2(C_{15}H_{12}N_2OOCH_3)]$ may be assigned to υ(C–O), indicating the presence of $–OCH_3$ in the complexes. The signal due to υ(O–H) (originally present at ~3080 cm^{-1} in free pyrazolines) is missing from spectra of the complexes, indicating deprotonation of the phenolic oxygen, further substantiated by the appearance of a band at 633–610 cm^{-1} that may be due to υ(Fe–O). IR spectra of iron(III) complexes are consistent with IR spectra of iron(III) pyrazolinates [26]. Thus, pyrazolines are bidentate ligands in these iron(III) complexes.

New bands in IR spectra of these iron(III) complexes (in comparison to iron(III) pyrazolinates) at 1179–1152 cm^{-1} and 974–955 cm^{-1} have been assigned to υ[(P)–O–C] and υ[P–O–(C)], respectively [32–37].

The υ[P=S] may be characterized by bands at 682–659 cm^{-1} and, in comparison with the spectra of the parent alkylenedithiophosphoric acid, there is shifting to lower frequency. This shift indicates bonding of thiophosphoryl sulfur to metal [37]. Bands at 560–550 cm^{-1} may be ascribed to υ[P–S]; new bands (in comparison to free ligand) at 361–335 cm^{-1} have been assigned to υ[Fe–S] [24] (table 4).

5.7. *FAB mass spectral studies*

The molecular weight of $Fe(C_6H_{14}O_2PS_2)(C_{15}H_{12}N_2OX)_2$ and $Fe(C_6H_{14}O_2PS_2)_2(C_{15}H_{12}N_2OX)$ have been determined by FAB mass spectra. FAB mass spectrometry is one of the most useful analytical techniques for structural elucidation of complexes. FAB mass spectra of all the compounds have been carried out and major fragments of the compounds are given in table 5. The main fragments of the free pyrazolines are at *m/z* 238, 146, 95, 93, and 70 due to $C_{15}H_{12}N_2OH$, $C_9H_{10}N_2$, C_6H_7O, C_6H_5O, and $C_3H_6N_2$, respectively. The main fragment of dithiophosphoric acid is at *m/z* 86 due to C_6H_{14}. The molecular ion peak clearly indicates that all the complexes are monomeric.

Table 5. FAB mass spectral data for $Fe(C_6H_{14}O_2PS_2)(C_{15}H_{12}N_2OX)_2$ and $Fe(C_6H_{14}O_2PS_2)_2(C_{15}H_{12}N_2OX)$.

Complex	Mol. wt. found (Calcd)	–py	–2py	–DTPA	–2DTPA	Fe_2O_3
$Fe(C_6H_{14}O_2PS_2)(C_{15}H_{12}N_2OH)_2$	742 (742.80)	506	268	530	–	160
$Fe(C_6H_{14}O_2PS_2)(C_{15}H_{12}N_2O{\cdot}OCH_3)_2$	802 (804.8)	534	267	587	–	160
$Fe(C_6H_{14}O_2PS_2)_2(C_{15}H_{12}N_2OCl)$	754 (753.30)	483	–	540	328	160
$Fe(C_6H_{14}O_2PS_2)_2(C_{15}H_{12}N_2OCH_3)$	733 (732.8)	484	–	519	305	160

Note: py = 3(2′-hydroxyphenyl)-5-(4-substituted phenyl) pyrazolines; DTPA = dithiophosphoric acid.

Table 6. Average diameter of particles for $Fe(C_6H_{14}O_2PS_2)(C_{15}H_{12}N_2OX)_2$ and $Fe(C_6H_{14}O_2PS_2)_2(C_{15}H_{12}N_2OX)$.

Complexes	2θ	Average* diameter (nm)	Average† diameter (nm)	Averagen diameter (nm)
$Fe(C_6H_{14}O_2PS_2)(C_{15}H_{12}N_2O{\cdot}OCH_3)_2$	44.81	85	475	90
$Fe(C_6H_{14}O_2PS_2)_2(C_{15}H_{12}N_2OCl)$	15.07	99	328	250

*Determined by XRD technique.
†Determined by SEM image analysis.
nDetermined by TEM image analysis.

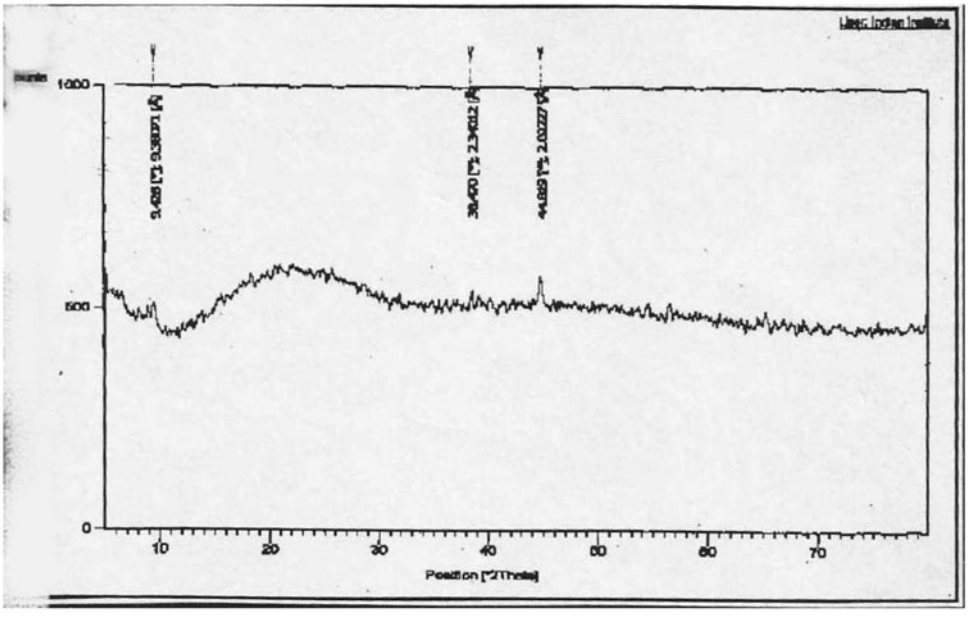

Figure 1. X-ray powder diffraction pattern of $Fe(C_6H_{14}O_2PS_2)(C_{15}H_{12}N_2O{\cdot}OCH_3)_2$.

5.8. *X-ray powder diffraction and electron microscopic studies*

The average diameter of the particle thus obtained was 85–120 nm. TEM studies showed that the particle size ranged from 90 to 250 nm. SEM studies showed that the particle size ranged from 190 to 540 nm. The morphology of $Fe(C_6H_{14}O_2PS_2)(C_{15}H_{12}N_2OX)_2$ and $Fe(C_6H_{14}O_2PS_2)_2(C_{15}H_{12}N_2OX)$ complexes were studied by employing XRD, SEM, and TEM techniques. The mean diameters of particles of the complexes are summarized in table 6. XRD powder diffraction pattern, SEM, and TEM image of $Fe(C_6H_{14}O_2PS_2)(C_{15}H_{12}N_2O{\cdot}OCH_3)_2$ are shown in figures 1–3, respectively. The particle size measured from XRD, SEM, and TEM for these iron(III) complexes are larger (90–525 nm) than the nanoparticle size.

5.9. *Cyclic voltammetry*

The redox properties of the complexes were followed by cyclic voltammetry using 0.1 M TBAP in acetonitrile as supporting electrolyte. The cyclic voltammetry of the complexes $[Fe(C_6H_{14}O_2PS_2)(C_{15}H_{12}N_2O{\cdot}OCH_3)_2]$ features the reduction of iron(III) to iron(II) at a cathodic peak potential of −0.360 V and oxidation of the iron(II) species at an anodic peak potential of +0.660 V.

Separation between the anodic and cathodic peak potential, $\Delta E_p = 1.02$ V, indicates an irreversible, one-electron redox process. The average peak potential for this compound was $E_{1/2} = 0.15$ V (figure 4).

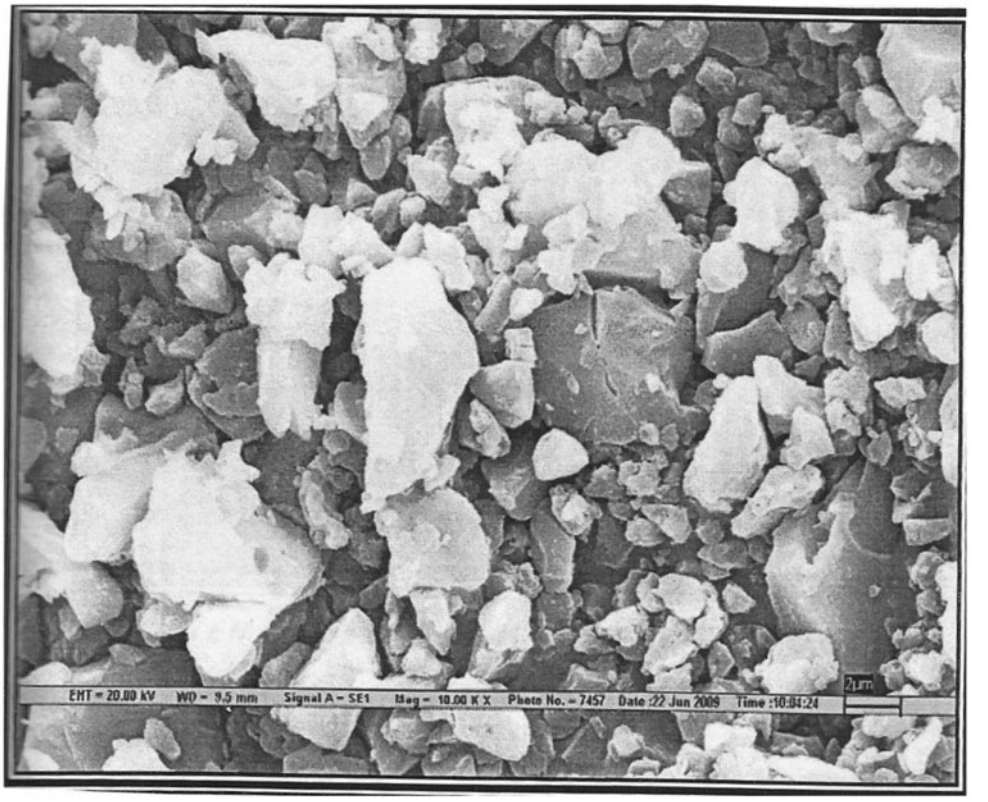

Figure 2. SEM image of $Fe(C_6H_{14}O_2PS_2)(C_{15}H_{12}N_2O{\cdot}OCH_3)_2$.

5.10. *Microbial assay*

The antimicrobial activity of free ligand and complexes were tested against two bacterial species *Bacillus subtilis* and *Pseudomonas* and two fungal species *Aspergillus flavus* and *Penicillium chrysogenum*, and their activities were compared with a commercial antibiotic Kanamycin and a commercial antifungal agent Terbinafin. The experiments were repeated and the results listed in table 7 are averages of three replicates.

$Fe(C_6H_{14}O_2PS_2)(C_{15}H_{12}N_2OX)_2$ and $Fe(C_6H_{14}O_2PS_2)_2(C_{15}H_{12}N_2OX)$ exhibit greater antibacterial effect towards *B. subtilis* and *Pseudomonas species* as compared to free pyrazoline and the known antibiotic agent Kanamycin (figure 5).

$Fe(C_6H_{14}O_2PS_2)(C_{15}H_{12}N_2OX)_2$ and $Fe(C_6H_{14}O_2PS_2)_2(C_{15}H_{12}N_2OX)$ also exhibit greater antifungal effects towards *A. flavus* and *P. chrysogenum* compared to free pyrazoline and Terbinafin (figure 6).

The results shown in table 7 indicate that $Fe(C_6H_{14}O_2PS_2)(C_{15}H_{12}N_2OX)_2$ and $Fe(C_6H_{14}O_2PS_2)_2(C_{15}H_{12}N_2OX)$ exhibit greater antibacterial and antifungal activity against all the pathogens tested, compared to pyrazolines and commercial antibiotic and antifungal agents, respectively. Thus, the complexes may be used as precursors of antibiotic and antifungal drugs after testing *in vitro*.

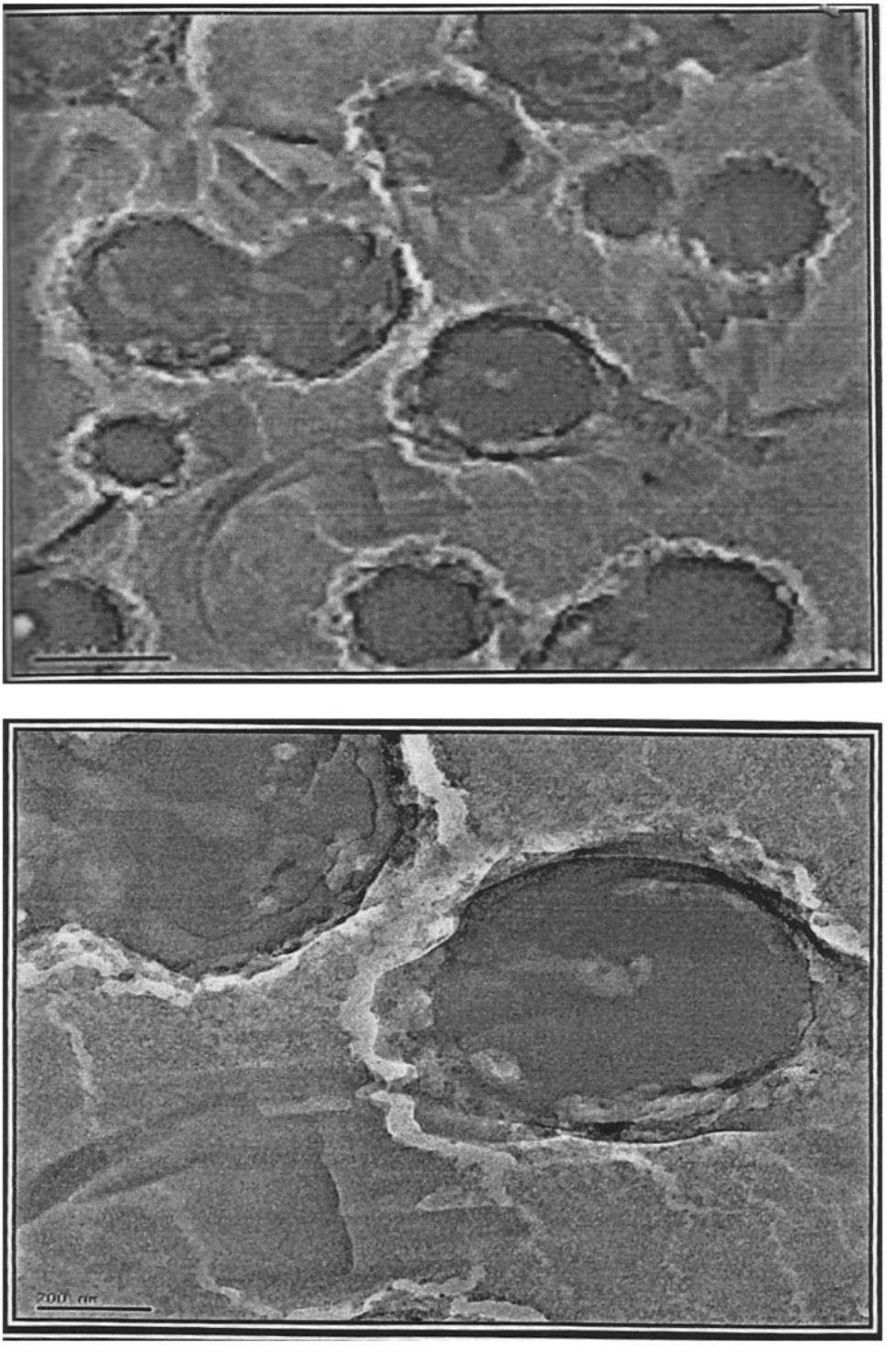

Figure 3. TEM image of $Fe(C_6H_{14}O_2PS_2)(C_{15}H_{12}N_2O{\cdot}OCH_3)_2$.

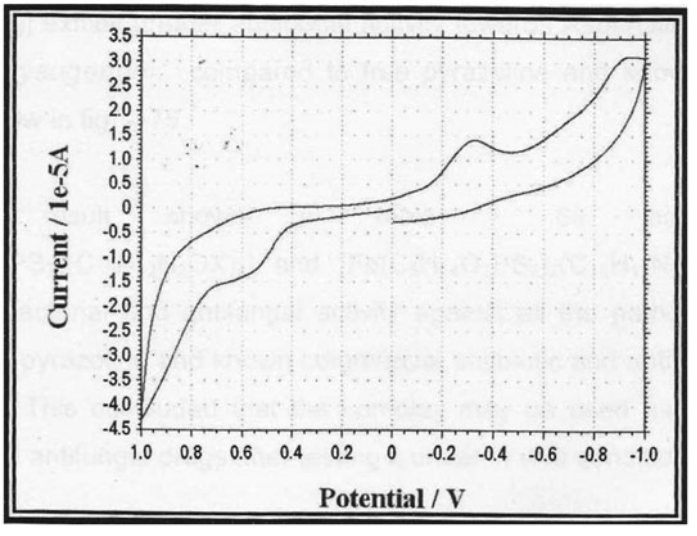

Figure 4. Cyclic voltammogram of $Fe(C_6H_{14}O_2PS_2)(C_{15}H_{12}N_2O{\cdot}OCH_3)$.

Table 7. Antimicrobial activity of $Fe(C_6H_{14}O_2PS_2)(C_{15}H_{12}N_2OX)_2$ and $Fe(C_6H_{14}O_2PS_2)_2(C_{15}H_{12}N_2OX)$.

	Fungi		Bacteria	
Comp. no.	*A. flavus*	*P. chrysogenum*	*B. subtilis* (G^+)	*Pseudomonas* sp. (G^-)
1	6	7	8	8
2	17	19	17	18
3	18	23	24	23
4	25	24	25	22
5	18	24	23	18
6	24	19	22	23

Notes: Diameter of inhibition zone measured in mm, article disk 5 mm, inhibition zone measured excluding article disk diameter with error limit ±0.5, amount of complexes taken 1 mg mL^{-1} of DMSO. The standards are in the form of sterile Hi-Disk cartridges, each disk containing 30 µm of the drug. 1 = 3(2′-hydroxyphenyl)-5-(4-substituted phenyl) pyrazolines, 2 = Terbinafin (antifungal agent) and Kanamycin (antibacterial agent), 3 = $[Fe(C_6H_{14}O_2PS_2)(C_{15}H_{12}N_2OH)_2]$, 4 = $[Fe(C_6H_{14}O_2PS_2)(C_{15}H_{12}N_2O{\cdot}OCH_3)_2]$, 5 = $[Fe(C_6H_{14}O_2PS_2)_2(C_{15}H_{12}N_2OCl)]$, and 6 = $[Fe(C_6H_{14}O_2PS_2)_2(C_{15}H_{12}N_2OCH_3)]$.

Free pyrazoline shows less activity but the complex with iron(III) enhances activity. Of the complexes of iron(III) pyrazolinates, methoxy substituted complexes show the highest activity against *A. flavus* [38].

All of our complexes $[Fe(C_6H_{14}O_2PS_2)(C_{15}H_{12}N_2OX)_2]$ and $[Fe(C_6H_{14}O_2PS_2)_2(C_{15}H_{12}N_2OX)]$ show higher activity against *B. subtilis* and *Pseudomonas* sp. than any other complexes of iron reported by us [16, 38, 39]. Complexes of iron(III) with pyrazoline and dithiophosphoric acid and with pyrazoline and aspartic acid show comparable activity against *P. chrysogenum* [16].

Ligands with nitrogen and oxygen donors inhibit enzyme activity, since the enzyme which requires these groups for their activity appears to be more susceptible to deactivation by metal ions on coordination. Moreover, coordination reduces the polarity of the metal ion because of partial sharing of its positive charge with the donor groups within the chelate ring system formed during coordination [40, 41].

Figure 5. Antibacterial activity against *B. subtilis* of $Fe(C_6H_{14}O_2PS_2)(C_{15}H_{12}N_2OH)_2$, where 1 – Solvents, 2 – Kanamycin, 3 – Complex, and 4 – 3(2′-hydroxy phenyl)-5-(4-phenyl) pyrazoline.

Figure 6. Antifungal activity against *A. flavus* of $Fe(C_6H_{14}O_2PS_2)(C_{15}H_{12}N_2OH)_2$, where 1 – 3(2′hydroxy phenyl)-5-(4-phenyl) pyrazolines, 2 – Terbinafin, 3 – Solvent, and 4 – Complex.

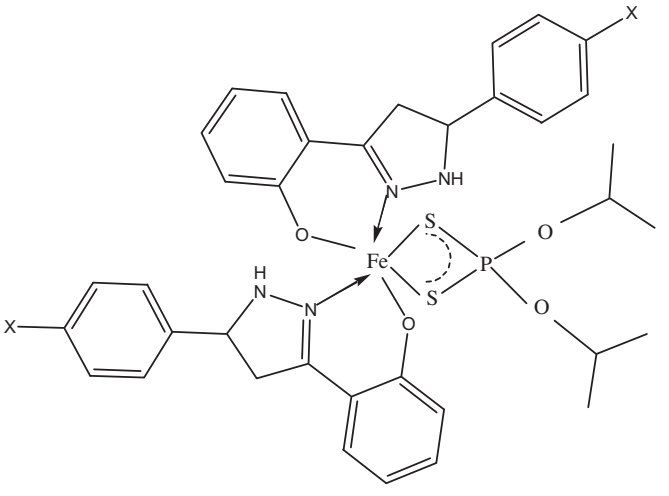

Figure 7. Proposed structure of $Fe(C_6H_{14}O_2PS_2)(C_{15}H_{12}N_2OX)_2$.

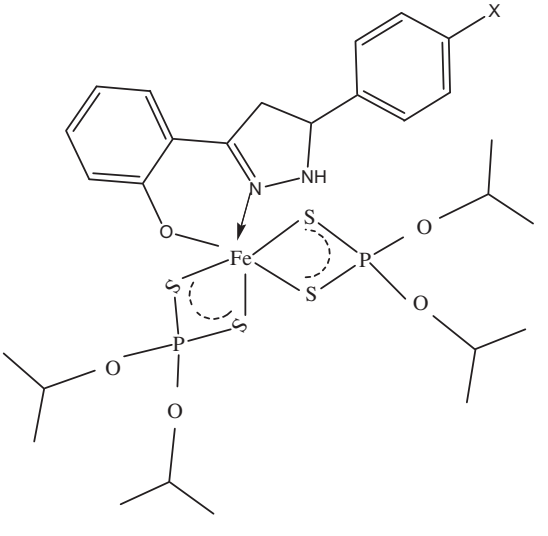

Figure 8. Proposed structure of $Fe(C_6H_{14}O_2PS_2)_2(C_{15}H_{12}N_2OX)$.

6. Conclusion

The present study describes a series of complexes $[Fe(C_6H_{14}O_2PS_2)(C_{15}H_{12}N_2OX)_2]$ and $[Fe(C_6H_{14}O_2PS_2)_2(C_{15}H_{12}N_2OX)]$; the monobasic bidentate behavior of the pyrazolines and bidentate behavior of dithiophosphoric acid in these complexes have been confirmed by IR

spectra. FAB mass spectra reveal the monomeric nature of the complexes. Electronic spectral data indicate octahedral geometry [24] around iron(III) (figures 7 and 8).

Magnetic moment measurements and molar conductance studies suggest that these are high-spin complexes and non-electrolytes.

XRD, TEM, and SEM studies suggest that the particle size of these complexes is in the nano-range. Cyclic voltammetry indicates that these complexes have irreversible redox properties.

Antimicrobial activities show that these complexes exhibit greater antibacterial and antifungal activities compared to pyrazoline and commercial antibiotic and antifungal agents, respectively. Because of significant antimicrobial activities of these complexes, they have been used as precursors of antibiotic and antifungal drugs after testing *in vitro*. The structure-activity relationship of iron complexes of the type $[Fe(C_6H_{14}O_2PS_2)(C_{15}H_{12}N_2OX)_2]$ and $[Fe(C_6H_{14}O_2PS_2)_2(C_{15}H_{12}N_2OX)]$ shows that methoxy-substituted pyrazoline has the maximum antibacterial and antifungal activity. All of our complexes $[Fe(C_6H_{14}O_2PS_2)(C_{15}H_{12}N_2OX)_2]$ and $[Fe(C_6H_{14}O_2PS_2)_2(C_{15}H_{12}N_2OX)]$ show higher activity against *B. subtilis* and *Pseudomonas* sp. in comparison to complexes of iron(III) with pyrazolines [38], ethylene glycol, and pyrazolines [39], as well as with pyrazolines and aspartic acid [16]. If we consider activity against *P. chrysogenum*, the complexes show comparable activity to complexes of iron(III) with pyrazoline and aspartic acid [16]. In many cases, metal complexes of ligands which have biological activity are more active than free ligands [42, 43] and our complexes also show much more activity than the free pyrazolines [38]. The activity of some antimicrobial drugs is dependent upon the complexing ability of the drugs with metal ions. Metal complexes of the drugs are often more lipophilic than the drugs themselves and thus facilitate transportation of the drugs across the cell membrane. For antibacterial and antifungal activities, it is often advantageous if the metal chelate is lipid soluble so that penetration of the cell is enhanced [44].

Acknowledgements

The authors are thankful to SAIF, CDRI, Lucknow (India), Punjab University, Chandigarh; Delhi University, IIT Delhi and BHU, Varanasi (India) and Department of Chemistry, DDU Gorakhpur University for providing the necessary spectral and analytical data.

References

[1] R.G. Mastin. U.S. 2, 25 A075 Nov, 16 (1961), *Chem. Abstr.*, **43**, 11782 (1983).
[2] J.R. Shah, N.R. Shah. *Ind. J. Chem.*, **A21**, 312 (1982).
[3] J.R. Shah, S.K. Das, R.P. Patel. *J. Ind. Chem. Soc.*, **50**, 228 (1973).
[4] N.R. Shah, J.R. Shah. *J. Inorg. Nucl. Chem.*, **43**, 1593 (1981).
[5] Fuji Photo Film Ltd; Jpn., Kokai Tokyo, Japan, 81, 40, 825. *Chem. Abstr.*, **96**, 190611 (1982).
[6] G. Kleefild, S. Dulzmann, EP 409,026 (Ci.C07D-231/06) (1991).
[7] D.J. Greenblat, S. Halder. *Benzodiazepines in Clinical Practice*, p. 18, North Holland Publishing Corp., Amsterdam (1974).
[8] U.N. Tripathi, J.S. Solanki. *J. Coord. Chem.*, **62**, 636 (2009).
[9] U.N. Tripathi, J.S. Solanki, A. Bhardwaj, T.R. Thapak. *J. Coord. Chem.*, **61**, 4025 (2008).
[10] U.N. Tripathi, M. Safi Ahmad, J.S. Solanki, A. Bhardwaj, A. Siddiqui. *Turk. J. Chem.*, **33**, 257 (2009).
[11] U.N. Tripathi, G. Venubabu, M. Safi Ahmad, S.S.R. Kolisetty, A.K. Srivastava. *J. Appl. Organomet. Chem.*, **20**, 669 (2006).
[12] U.N. Tripathi, M. Safi Ahmad, G. Venubabu, D.R. Khate. *Main Group Met. Chem.*, **29**, 39 (2006).
[13] U.N. Tripathi, M. Safi Ahmad, G. Venubabu, P. Ramakrishna. *J. Coord. Chem.*, **60**, 1777 (2007).
[14] U.N. Tripathi, M. Safi Ahmad, G. Venubabu, P. Ramakrishna. *J. Coord. Chem.*, **60**, 1709 (2007).

[15] U.N. Tripathi, M. Safi Ahmad, G. Venubabu. *Turk J. Chem.*, **31**, 45 (2007).
[16] A. Siddiqui, K. Singh, K. Lata Singh, S. Gupta, M.S. Ahmad, U.N. Tripathi. *Appl. Organomet. Chem.*, **26**, 203 (2012).
[17] A.I. Vogel. *A Text Book of Quantitative Organic Analysis*, ELBS and Longman, London (1978).
[18] T.C. Sharma, V. Saxena, N.J. Reddy. *Acta Chim. (Budapest)*, **93**, 415 (1977).
[19] J.E. Drake, C.L.B. MacDonald, A. Kumar, S.K. Pandey, R. Ratnani. *J. Chem. Crystallogr.*, **35**, 447 (2005).
[20] A.I. Vogel. *A Text Book of Quantitative Inorganic Analysis*, ELBS and Longman, London (1985).
[21] A. Khan, M. Rahman, S. Islam. *Turk. J. Biol.*, **31**, 162 (2007).
[22] S. Dash, L.K. Nath, S. Bhise, N. Bhuyan. *Trop. J. Pharm. Res.*, **4**, 341 (2005).
[23] N.S. Youssef, E.A. El-Zahany, B.N. Barsoum, A.M.A. El-Seidy. *Transition Met. Chem.*, **34**, 905 (2009).
[24] U.N. Tripathi, G. Srivastava, R.C. Mehrotra. *Transition Met. Chem.*, **19**, 564 (1994).
[25] U.N. Tripathi, K.V. Sharma, A. Chaturvedi, T.C. Sharma. *Polish J. Chem.*, **77**, 109 (2003).
[26] U.N. Tripathi, K.V. Sharma, V. Sharma. *J. Coord. Chem.*, **61**, 3314 (2008).
[27] C.J. Ballhausen. *Introduction to Ligand Field Theory*, McGraw-Hill Book Company, New York (1962).
[28] M. Revanasiddappa, T. Suresh, S. Khasim, S.C. Raghavendray, C. Basavaraja, S.D. Angadi. *E. J. Chem.*, **5**, 395 (2008).
[29] N. Saha, D.K. Sau. *Transition Met. Chem.*, **30**, 532 (2005).
[30] R.M. Silverstein, F.X. Webster. *Spectrometric Identification of Organic Compounds*, 6th Edn, John Wiley & Sons Inc., New York (1998).
[31] K. Nakamoto. *Infrared and Raman Spectra of Inorganic and Coordination Compounds*, Wiley Interscience, New York (1997).
[32] U.N. Tripathi, R. Mirza, M. Safi Ahmad. *Phosphorus, Sulphur Silicon*, **182**, 1291 (2007).
[33] U.N. Tripathi, M. Safi Ahmad, R. Mirza, A. Siddiqui. *Phosphorus, Sulphur Silicon*, **182**, 1 (2007).
[34] U.N. Tripathi, P.P. Bipin, R. Mirza, A. Chaturvedi. *Polish J. Chem.*, **73**, 1751 (1991).
[35] U.N. Tripathi, P.P. Bipin, R. Mirza, S. Shukla. *J. Coord. Chem.*, **55**, 1111 (2002).
[36] U.N. Tripathi, M.S. Ahmad. *J. Coord. Chem.*, **59**, 1583 (2006).
[37] (a) A.A. Khan, K. Iftikhar. *Polyhedron*, **16**, 4153 (1997); (b) A.A. Khan, K. Iftikhar. *Chem. Abstr.*, **128**, 28153 (1997).
[38] K.V. Sharma, V. Sharma, U.N. Tripathi. *J. Coord. Chem.*, **61**, 3314 (2008).
[39] U.N. Tripathi, M.S. Ahmad, A. Siddiqui, K. Singh. *J. Coord. Chem.*, **63**, 894 (2010).
[40] Z.H. Chohan, C.T. Supuran, A. Scozzafava. *J. Enzyme Inhib. Med. Chem.*, **19**, 79 (2004).
[41] B.N. Meyer, N.R. Ferrigni, J.E. Putnam, L.B. Jacobsen, D.E. Nichols, J.L. McLaughlin. *Planta Med.*, **45**, 31 (1982).
[42] S. Kirschner, Y.K. Wei, D. Francis, J.G. Bergman. *J. Med. Chem.*, **9**, 369 (1966).
[43] A.J. Thomson, R.J.P. Williams, S. Reslova. *Structure and Bonding*, Vol. 11, Springer-Verlag, New York (1972).
[44] P.M. Harrison, R.J. Hoare. *Metals in Biochemistry*, Chapman and Hall, London (1980).